nature photonics

ARTICLES

PUBLISHED ONLINE: 7 AUGUST 2011 | DOI: 10.1038/NPHOTON.2011.168

# Sensitive mid-infrared detection in wide-bandgap semiconductors using extreme non-degenerate two-photon absorption

Dmitry A. Fishman[1‡], Claudiu M. Cirloganu[1†‡], Scott Webster[1], Lazaro A. Padilha[1†], Morgan Monroe[1], David J. Hagan[1,2] and Eric W. Van Stryland[1,2]*

**Identifying strong and fast nonlinearities for today's photonic applications is an ongoing effort[1]. Materials[2–5] and devices[6–9] are typically sought to achieve increasing nonlinear interactions. We report large enhancement of two-photon absorption through intrinsic resonances using extremely non-degenerate photon pairs. We experimentally demonstrate two-photon absorption enhancements by factors of 100–1,000 over degenerate two-photon absorption in direct-bandgap semiconductors. This enables gated detection of sub-bandgap and sub-100 pJ mid-infrared radiation using large-bandgap detectors at room temperature. Detection characteristics are comparable in performance to liquid-nitrogen-cooled HgCdTe (MCT) detectors. The temporal resolution of this gated detection by two-photon absorption is determined by the gating pulse duration.**

Semiconductors are excellent materials for photonic switching because of their large third-order nonlinearities, and have been the subject of extensive studies, both experimental and theoretical[10,11]. These nonlinearities, both refractive and absorptive, have been successfully modelled and experimentally verified in many material-wavelength combinations[12–14]. However, little attention has been paid to theoretical predictions for the case where the input wavelengths are vastly different. Consequently, before the present study, no efforts had been made to study extreme non-degenerate two-photon absorption (ND-2PA) experimentally. A theoretical treatment of ND-2PA in direct-bandgap semiconductors using two parabolic bands has shown that ND-2PA may be expressed by[15]

$$\frac{\mathrm{d}I_1}{\mathrm{d}z} = -2\alpha_2(\omega_1;\omega_2)I_2I_1$$

$$\text{with} \qquad \alpha_2(\omega_1;\omega_2) = K\frac{\sqrt{E_\mathrm{p}}}{n_1 n_2 E_\mathrm{gap}^3}F_2\left(\frac{\hbar\omega_1}{E_\mathrm{gap}};\frac{\hbar\omega_2}{E_\mathrm{gap}}\right) \qquad (1)$$

where

$$F_2(x_1;x_2) = \frac{(x_1+x_2-1)^{3/2}}{2^7 x_1 x_2^2}\left(\frac{1}{x_1}+\frac{1}{x_2}\right)^2$$

$\alpha_2(\omega_1;\omega_2)$ is the ND-2PA coefficient for optical frequencies $\omega_{1,2}$ and their associated irradiances $I_{1,2}$, $E_\mathrm{p}$ is the Kane energy parameter, $E_\mathrm{gap}$ is the bandgap energy, $n_{1,2}$ are the refractive indices, and $K$ is a material independent parameter.

From the energy denominators in $F_2$, 2PA is expected to increase drastically if either $\omega_1$ or $\omega_2$ becomes small. As 2PA requires $\hbar\omega_1 + \hbar\omega_2 \geq E_\mathrm{gap}$, this means that 2PA increases with the ratio of photon energies. This can be qualitatively understood by noting that the allowed–forbidden transition scheme in perturbation theory dominates 2PA in direct-bandgap semiconductors, as shown by Wherrett[16]. Thus, the smaller energy photon is almost resonant to the intraband (or self) transition. The limits to this enhancement are dictated by the linear absorption of the higher energy photon as it approaches the linear absorption resonance. Hence, the degenerate 2PA (D-2PA) case gives the minimum 2PA, and can only be enhanced by using the $E_\mathrm{gap}^{-3}$ dependence in equation (1). This results in the use of narrow-bandgap semiconductors and thus mid-infrared (MIR) wavelengths. This $E_\mathrm{gap}^{-3}$ dependence was verified experimentally, revealing D-2PA coefficients for narrow-bandgap semiconductors such as InSb that are three orders of magnitude larger than for large-bandgap semiconductors such as ZnSe[12,13,17]. The use of extremely non-degenerate photons in wide-bandgap materials results in 2PA coefficients similar to those obtained using degenerate photons in narrow-bandgap materials. These enhancements observed for extreme ND-2PA should also apply to other material systems provided that the linear absorption band edge is sufficiently sharp[18–20].

The large increase in 2PA for extreme non-degenerate configurations can be applied in a variety of ways. One of the most straightforward effects of the simultaneous absorption of two largely different photon energies is the promotion of a free carrier into the conduction band. One can monitor the photo-generated charges in such experiments using a 'gating' pulse, where this pulse can be composed of either high- or low-energy photons. We use the word 'gating' because this intense pulse essentially turns the detector on to monitor the intensity of the 'signal' pulse. If the gating pulse consists of low-energy photons, such experiments enable high-sensitivity detection of sub-bandgap-energy photons. Alternatively, a gating pulse comprising high-energy photon pulses (but still below the band edge) allows the detection of MIR photons using a large-bandgap semiconductor.

[1]CREOL, the College of Optics & Photonics, University of Central Florida, 4000 Central Florida Blvd., Orlando, Florida 32816-2700, USA, [2]Department of Physics, University of Central Florida, 4000 Central Florida Boulevard, Orlando, Florida 32816, USA; [†]Present address: COPE, Center for Organic Photonics and Electronics, School of Electrical and Computer Engineering, Georgia Institute of Technology, Atlanta, Georgia 30332, USA, Los Alamos National Laboratory, PO Box 1663, Los Alamos, NM 87545, USA (L.A.P.); [‡]These authors contributed equally to this work. *e-mail: ewvs@creol.ucf.edu

Figure 1a shows the detection of femtosecond pulses at 390 nm (3.18 eV) by a conventional GaN detector with $E_{gap} = 3.28$ eV (direct output voltage) using MIR gating pulses at 5.6 μm (6.7% of $E_{gap}$) (see Supplementary Information for details). The signal, which is proportional to the photo-generated carrier density $N$, is linear in both the MIR and ultraviolet (UV) beam irradiances, and is given by

$$\frac{dN}{dt} = 2\alpha_2(\omega_s;\omega_g)I_gI_s/\hbar\omega_s = 2\alpha_2(\omega_g;\omega_s)I_gI_s/\hbar\omega_g$$
$$= K\frac{\sqrt{E_p}}{n_1 n_2 E_g^4}F_2^{symm}\left(\frac{\hbar\omega_s}{E_g};\frac{\hbar\omega_g}{E_g}\right)2I_sI_g \quad (2)$$

with $F_2^{symm}(x_1; x_2)$ given by

$$F_2^{symm}(x_1;x_2) = \frac{(x_1+x_2-1)^{3/2}}{2^7(x_1x_2)^2}\left(\frac{1}{x_1}+\frac{1}{x_2}\right)^2$$

where $I_s$, $\hbar\omega_s$ and $I_g$, $\hbar\omega_g$ are irradiances and photon energies of signal and gating pulses, respectively. We introduce $F_2^{symm}(x_1; x_2)$ to explicitly show that although the 2PA coefficients are not symmetric in the two input frequencies, the detected carrier density is symmetric in these frequencies, so the signal enhancement is the same for gated detection of MIR and UV light.

The measured detector responsivity $R$ (5.6 μm; @ 0.5 GW cm$^{-2}$) is >0.034 A W$^{-1}$ (additional detector parameters are found in the Supplementary Information). These results are linearly dependent on the irradiance at 5.6 μm (~0.5 GW cm$^{-2}$) as the effective 'linear' absorption is $\alpha_2(\omega_s; \omega_g)I_g$. Corresponding 730 nm pulses of approximately the same pulse energy as the UV pulses yield a D-2PA signal voltage that is nearly three to four orders of magnitude smaller (indicated by the results in Fig. 1a).

We can also detect weak 5.6 μm by increasing the irradiance of the 390 nm pulses to act as a gate. Thus a wide-bandgap semiconductor ($E_{gap} = 3.28$ eV) can be used for the detection of MIR light of photon energy 0.22 eV (5.6 μm). However, the cross absorption term is now accompanied by the D-2PA of the 390 nm pulses, $\alpha_2(\omega_g; \omega_g)$,

$$dN/dt = \alpha_2(\omega_g;\omega_g)I_g^2/2\hbar\omega_g + 2\alpha_2(\omega_s;\omega_g)I_gI_s/\hbar\omega_s \quad (3)$$

where the signal is 5.6 μm and the gate is 390 nm. The calculated values of D- and ND-2PA, $\alpha_2(\omega_{390nm}; \omega_{390nm})$, and $\alpha_2(\omega_{5600nm}; \omega_{390nm})$, $\alpha_2(\omega_{390nm}; \omega_{5600nm})$ are 2.2 cm GW$^{-1}$, 17 cm GW$^{-1}$, and 240 cm GW$^{-1}$, respectively. This gives a ratio for the IR gating of 110, whereas the measured ratio is 95. The D-2PA signal can be suppressed for repetitive pulses using the modulation of the MIR pulses and lock-in detection, easily allowing for the detection of sub-100 pJ pulse energies at 5.6 μm (see Supplementary Information). This is shown in Fig. 1b, where we demonstrate 5.6 μm detection using a GaN detector at room temperature. We compare the signals with gated detection in GaN using several 390 nm pulse energies with the output voltage from a conventional liquid-nitrogen-cooled mercury cadmium telluride (MCT) detector. The results show comparable or even superior performance for the investigated detectors (see Supplementary Information for details).

There are a few salient facts that need to be stressed regarding these experiments. As seen in Fig. 1, we are able to directly compare signals obtained when measuring MIR wavelengths using either one-photon or two-photon processes. It is obvious that when using a linear process, the responsivity depends solely on the overall linear absorption of the material used (that is, $\alpha L$), where $\alpha$ is the linear absorption coefficient and $L$ is detector element thickness. In the ND-2PA case, the effective absorption coefficient is $2\alpha_2 I_g$. In both cases we desire the overall thickness to be greater than the absorption depth. We estimate for the experiments demonstrated here that we are well away from this limit (~2% loss in the active detector region), and there is considerable optimization that can be performed. Also, because we do not

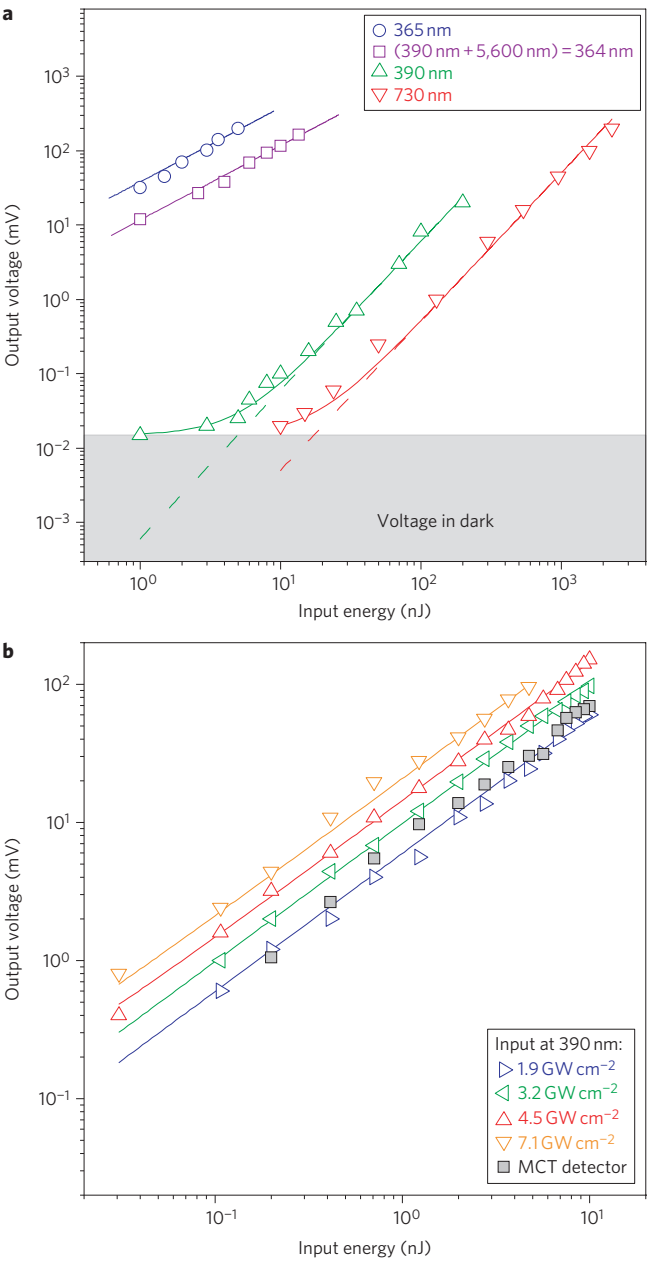


**Figure 1 | Mid-IR detection using a UV photodiode. a**, Log–log plot of the output voltage of a GaN diode versus 390 nm (3.18 eV, 100 fs) input signal energy in the presence of temporally overlapped, 300 nJ, 215 fs, 5.6 μm (0.22 eV) gating pulses. Also shown are outputs versus 365 nm (linear response) (100 fs), 390 nm without the gating pulses and signal from D-2PA of 730 nm (1.70 eV, 110 fs) pulses. Lines are fits to either slope 1 (for a linear dependence) or 2 (for a quadratic dependence) with ~15 μV of dark voltage. **b**, Log–log plot of the output voltage of a GaN diode versus 5.6 μm (215 fs) input signal energy in the presence of temporally overlapped 390 nm gating pulses (100 fs) of various energies. The grey filled squares show data for the MCT detector. See Supplementary Information for detector specifications.

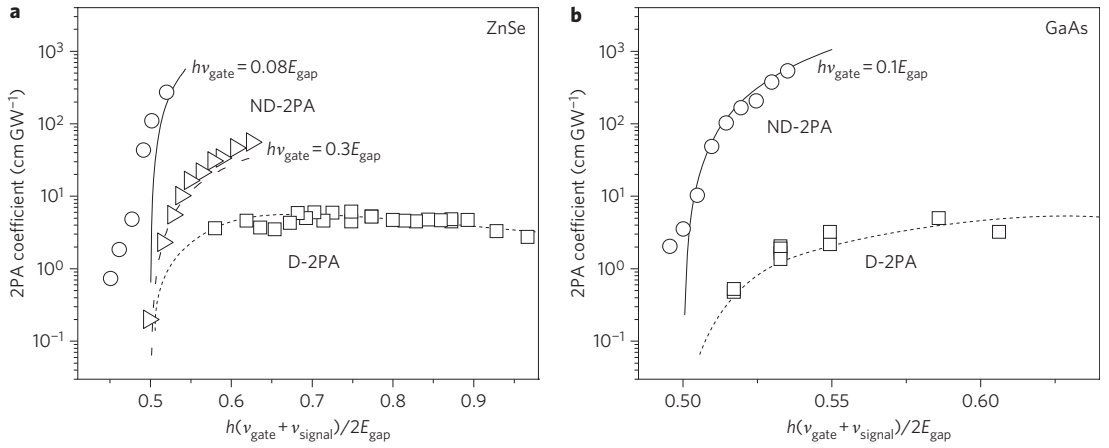


**Figure 2 | Extreme ND-2PA in semiconductors. a**, Femtosecond pump (gate)–probe (signal) results: D- and ND-2PA coefficient of ZnSe ($E_{gap} = 2.67$ eV) versus the sum of pump and probe photon energies normalized to the bandgap: theory (lines). **b**, Picosecond pump–probe results: D- and ND-2PA coefficients of GaAs ($E_{gap} = 1.42$ eV).

require high-speed detection, thick materials including waveguide geometries could be helpful.

In 2PA detection one preserves the signal linearity while having direct control of the responsivity via the gating pulse irradiance $R = A{\cdot}I_g$, where $A = 7.1 \times 10^{-12}$ cm$^2$ A W$^{-2}$ for the 390 nm gating pulse ($A = 6.8 \times 10^{-11}$ cm$^2$ A W$^{-2}$ for the MIR gating pulse). This offers flexibility for some applications that can outweigh the necessity of having a gating pulse. One can then measure pulsed low-energy MIR radiation using room-temperature detectors with a user-controlled responsivity. Also, even though the results of these experiments are related to the particular material and wavelength pair, the same approach can be used to measure any other pair of wavelengths using a material with appropriate bandgap energy. The bandwidth is determined by a trade-off with the 2PA enhancement, as will be seen from the transmittance experiments described in the next paragraph. One possible concern is the current created through direct D-2PA. However, the D-2PA is not enhanced; therefore, for practical applications the irradiance levels needed for the gate pulse should not lead to saturation effects. For MIR detection, the D-2PA of the gating pulse appears as a background signal. In our experiments, amplitude noise on the gating laser pulse dominates the contributions to noise. Noise from the gated signal is linear in the gate irradiance, whereas the degenerate 2PA noise is quadratic in the gate irradiance. There is therefore a trade-off between responsivity, which is linear in the gate irradiance, and this noise, which can have linear or quadratic contributions (Fig. 1). This is analogous to having a 'noisy' detector electronic amplifier; however, this 'noise' is measurable and could in principle be calibrated out. For this reason, we do not quote a noise-equivalent power or $D^*$ for this detection scheme. However, the minimum detectable energy (Fig. 1b) is ~20 pJ, whereas for MCT the minimum detectable energy is ~200 pJ (for details of detector parameters, such as pre-amplifier and transimpedance gain, see Supplementary Information). This difference is in large part due to the fact that we can use modulation techniques with the ND-2PA gated detection scheme.

An alternative to this new detection method is frequency upconversion using second-order nonlinear optical materials in which IR and visible/near-IR photons are summed to yield photons of sufficient energy to be used with high-quantum-efficiency detectors such as silicon[21–23]. The primary similarity is that both detection schemes result in photocarrier densities proportional to the product of gate and signal irradiances. However, upconversion requires phase-matched second-order nonlinear materials. After years of development, it has resulted in near-unity detection quantum efficiencies[24–26]. The ND-2PA method demonstrated here is considerably simpler, because the detector element itself is the nonlinear material and no phase-matching is required; however, considerable research and development is necessary for it to reach its ultimate limits.

To provide a quantitative picture we performed detailed transmission studies of the direct-bandgap semiconductors ZnSe and GaAs using various photon energy ratios and picosecond and femtosecond pulses. In these experiments, the transmittance of weak visible pulses was monitored in the presence of intense MIR pulses (see Supplementary Information). 2PA coefficients for ZnSe and GaAs at different photon energy ratios are presented in Fig. 2a and b, respectively. Large enhancements of ND-2PA values versus D-2PA values were obtained, by as much as 270× in ZnSe (photon energy ratio up to 12.5, Fig. 2a) and 127× in GaAs (photon energy ratio of 10, Fig. 2b). For these semiconductors, the experimental results agree with theory, except for deviations observed when the sum of photon energies is less than the bandgap. This exception is probably due to absorption in the Urbach tail[27].

This greatly enhanced 2PA should enable many new opportunities beyond detection, such as all-optical switching[28] using microring resonators[29], and waveguides[30] with direct-bandgap semiconductors such as GaAs[31], where the resonating light is just below the band edge. Here the cavity $Q$ can be easily spoiled using IR pulses via ND-2PA. Gated detection has also been suggested for quantum detectors[32,33]. The enhancement noted here makes these much more attractive. Finally, we note that this very large enhancement of 2PA in the case of non-degenerate photons implies that two-photon gain[34] should show a similar enhancement with non-degeneracy. Experiments have shown two-photon emission of very non-degenerate photons.

The application to sub-bandgap detection in the commercial GaN detector studied here is far from optimized for the detection of extremely non-degenerate photons. For example, the ND-2PA could be significantly increased by using a thicker detector element to efficiently absorb the radiation. The intrinsic detector temporal response is irrelevant, because the speed of detection is determined by the gating pulsewidth. In addition, an ultralow-noise optical comb source could be used as the gating source, which would greatly improve the signal-to-noise ratio[35].

## Methods

The experimental ND-2PA data presented in this Article were taken in a standard pump–probe non-collinear geometry with a small angle (~10°) between the pump and probe beams, using either picosecond or femtosecond pulses. A Ti:sapphire

laser system (ClarkMXR, CPA 2010) was used as a source of femtosecond pulses, producing ~1.4 mJ, ~150 fs (FWHM), 780 nm pulses at a repetition rate of 1 kHz. The output of the laser system was divided into two pulses by a beamsplitter. A portion of the 780 nm light was used to pump an optical parametric generator/amplifier (OPG/A, TOPAS-800, Light Conversion) to generate MIR pulses. For the near-IR (1.7–2.5 μm, used for transmission experiments) an idler pulse was used, but for longer wavelengths we used difference frequency generation (DFG) of signal and idler pulses. The irradiance of the IR pulses was controlled by a calibrated pair of $BaF_2$ wire-grid polarizers (Specac). The remainder of the 780 nm output was temporally delayed and used either to generate a weak white-light continuum (WLC, used as a probe for bulk semiconductor measurements) or to generate an intense second harmonic (390 nm) and used as a strong pump pulse for gated detector measurements. WLC was generated either in water (1 cm cell) or in a 2-mm-thick piece of $CaF_2$. Individual wavelengths were selected from the WLC using a set of narrow band-pass interference filters (Melles Griot, CVI) with a spectral bandwidth of ~8 nm (FWHM). The temporal width of the spectrally filtered pulses was between 140 fs and 160 fs, as verified by autocorrelation measurements. Pulsewidths in the femtosecond MIR were determined from cross-correlation measurements to be ~215 fs (FWHM). In all ND-2PA experiments the MIR was modulated using a mechanical chopper at 283 Hz, synchronized with the repetition rate from the Ti:sapphire laser. A lock-in amplifier was then used to record the signals. This MIR modulation ensured that D-2PA did not contribute to the lock-in output.

A similar set-up was used for the picosecond experiments. A mode-locked Nd:YAG laser system (EKSPLA) produced ~30 ps (FWHM) pulses of 110 mJ at 1,064 nm and a repetition rate of 10 Hz. The fundamental pulses were converted to the third harmonic at 355 nm, which then pumped a lithium triborate, $LiB_3O_5$ (LBO)-based OPG/OPA. The MIR pump pulses were obtained using a DFG process, mixing 1,064 nm output from the laser and the idler pulse from a second similar OPG/OPA. The probe beam had a maximum energy of a few nanojoules and a spot size smaller than that of the pump, as measured by knife-edge scans. This assured an irradiance in the probe beam smaller (by at least a factor of 100) than that of the pump beam. This caused minimal losses from D-2PA of the probe (<0.5%, which is at our noise limit). Pulsewidths from the picosecond OPG/OPA were measured by pump–probe and cross-correlation experiments to be 10–13 ps (FWHM), depending on the spectral region.

For the femtosecond gated detection experiments, we used a conventional PIN GaN detector with an active area of 0.25 $mm^2$ and a total GaN thickness of 5 μm, as determined using focused ion beam instrument (FEI 200 TEM FIB) cutting and imaging, with p- and i-GaN regions estimated to be <1 μm in thickness[36]. This detector was used in photoconductive mode, with a preamplifier gain factor of 40 (transimpedance gain, $400 \times 10^3$ V $A^{-1}$) and a variable reverse bias voltage from 1 to 4 V. Measurements of extreme ND-2PA in the GaN detector element resulted in cross-correlation of MIR (5.6 μm @ 0.5 GW $cm^{-2}$) pulses with near-UV (390 nm) pulses (Supplementary Fig. S1). The experimental results yielded ~230 fs (FWHM) for the MIR pulses, assuming Gaussian temporal profiles. The detector response voltage presented in Fig. 1a (390 nm + 5.6 μm curve) was recorded at zero time delay between the MIR and UV pulses. The detection of MIR pulses at 5.6 μm using gating pulses at 390 nm of different irradiances is presented in Fig. 1b. The background signal from D-2PA of the 390 nm pulses was eliminated by modulation of the weak MIR signal and the use of lock-in detection. The calculated D-2PA coefficient for 390 nm was ~2.2 cm $GW^{-1}$, which is more than two orders of magnitude less than the ND-2PA of ~240 cm $GW^{-1}$.

A conventional liquid-nitrogen-cooled HgCdTe (MCT) detector (Electro-Optical Systems Inc., model MCT14-040-E-LN6; active area, 16 $mm^2$, noise equivalent power (NEP) = $23 \times 10^{-12}$ W $Hz^{-1/2}$, $D^* = 1.7 \times 10^{10}$ cm $Hz^{1/2}$ $W^{-1}$, $R = 7.8 \times 10^3$ V $W^{-1}$ @ preamp out, pre-amp gain of 100, transimpedance gain $5 \times 10^3$ V $A^{-1}$) was used in the experiments for comparison. As discussed, for the case of non-degenerate gated detection, the signal is linearly proportional to the gate pulse irradiance $R = A \cdot I_g$, where $A_{IR\ gate} = 6.8 \times 10^{-11}$ $cm^2$ A $W^{-2}$ and $A_{UV\ gate} = 7.1 \times 10^{-12}$ $cm^2$ A $W^{-2}$). As an example, the measured values are $R_{IR\ gate} = 0.034$ A $W^{-1}$ for 0.5 GW $cm^{-2}$ of 5.6 μm gate pulse irradiance, and $R_{UV\ gate} = 0.032$ A $W^{-1}$ for 4.5 GW $cm^{-2}$ of 390 nm gate pulse irradiance. Parameters used in the detection experiments and associated calculations[37–39] are given in Supplementary Table S1.

Received 4 April 2011; accepted 30 June 2011; published online 7 August 2011

## References


1. Haque, S. A. & Nelson, J. Toward organic all-optical switching. *Science* **327,** 1466–1467 (2010).
2. Yumoto, J. *et al.* Enhancement of optical nonlinearity of heavy-metal oxide glasses by replacing lead and bismuth with thallium. *Appl. Phys. Lett.* **63,** 2630–2632 (1993).
3. Sasaki, F., Kobayashi, S. & Haraichi, S. Enhancement of the optical nonlinearity in pseudoisocyanine J aggregates embedded in distributed feedback microcavities. *Appl. Phys. Lett.* **81,** 391–393 (2002).
4. Soljačić, M. & Joannopoulos, J. D. Enhancement of non-linear effects using photonic crystals. *Nature Mater.* **3,** 211–219 (2004).
5. Hales, J. M. *et al.* Design of polymethine dyes with large third-order optical nonlinearities and loss figures of merit. *Science* **327,** 1485–1488 (2010).
6. Genevet, P. *et al.* Large enhancement of nonlinear optical phenomena by plasmonic nanocavity gratings. *Nano Lett.* **10,** 4880–4883 (2010).
7. Schuller, J. A. *et al.* Plasmonics for extreme light concentration and manipulation. *Nature Mater.* **9,** 193–204 (2010).
8. Capasso, F., Sirtori, C. & Cho, A. Y. Coupled quantum well semiconductors with giant electric field tunable nonlinear optical properties in the infrared. *IEEE J. Quantum Electron.* **30,** 1313–1326 (1994).
9. Paiella, R. *et al.* Self-mode-locking of quantum cascade lasers with giant ultrafast optical nonlinearities. *Science* **290,** 1739–1742 (2000).
10. Tanabe, T., Notomi, M., Kuramochi, E., Shinya, A. & Taniyama, H. Trapping and delaying photons for one nanosecond in an ultrasmall high-*Q* photonic crystal nanocavity. *Nature Photon.* **1,** 49–52 (2007).
11. Christodoulides, D., Khoo, I. C., Salamo, G. J., Stegeman, G. I. & Van Straland, E. W. Nonlinear refraction and absorption: mechanisms and magnitudes. *Adv. Opt. Photon.* **2,** 60–200 (2010).
12. Said, A. A. *et al.* Determination of bound-electronic and free-carrier nonlinearities in ZnSe, GaAs, CdTe, and ZnTe. *J. Opt. Soc. Am. B* **9,** 405–414 (1992).
13. Hutchings, D. C. & Van Stryland, E. W. Nondegenerate two-photon absorption in zinc blende semiconductors. *J. Opt. Soc. Am. B* **9,** 2065–2074 (1992).
14. Sheik-Bahae, M., Wang, J., DeSalvo, R., Hagan, D. J. & Van Styland, E. W. Measurement of nondegenerate nonlinearities using a two-color z scan. *Opt. Lett.* **17,** 258–260 (1992).
15. Sheik-Bahae, M., Hutchings, D. C., Hagan, D. J. & Van Stryland, E. W. Dispersion of bound electronic nonlinear refraction in solids. *IEEE J. Quantum Electron.* **27,** 1296–1309 (1991).
16. Wherrett, B. S. Scaling rules for multiphoton interband absorption in semiconductors. *J. Opt. Soc. Am. B* **1,** 67–72 (1984).
17. Olszak, P. D. *et al.* Spectral and temperature dependence of two-photon and free-carrier absorption in InSb. *Phys. Rev. B* **82,** 235207 (2010).
18. Hales, J. M. *et al.* Resonant enhancement of two-photon absorption in substituted fluorine molecules. *J. Chem. Phys.* **121,** 3152–3160 (2004).
19. Pati, S. K., Marks, T. J. & Ratner, M. A. Conformationally tuned large two-photon absorption cross sections in simple molecular chromophores. *J. Am. Chem. Soc.* **123,** 7287–7291 (2001).
20. Kogej, T. *et al.* Mechanisms for enhancement of two-photon absorption in donor–acceptor conjugated chromophores. *Chem. Phys. Lett.* **298,** 1–6 (1998).
21. Kleinman, D. A. & Boyd, G. D. Infrared detection by optical mixing. *J. Appl. Phys.* **40,** 546–566 (1969).
22. Gurski, T. R., Epps, H. W. & Maran, S. P. Upconversion of broadband infrared spectra. *Appl. Opt.* **17,** 1238–1242 (1978).
23. Watson, E. A. & Morris, G. M. Comparison of infrared upconversion methods for photon-limited imaging. *J. Appl. Phys.* **67,** 6075–6084 (1990).
24. Hadfield, R. H. Single-photon detectors for optical quantum information applications, *Nature Photon.* **3,** 696–705 (2009).
25. Gu, X. *et al.* Temporal and spectral control of single-photon frequency upconversion for pulsed radiation, *Appl. Phys. Lett.* **96,** 131111 (2010).
26. Thew, R. T., Zbinden, H. & Gisin, N. Tunable upconversion photon detector. *Appl. Phys. Lett.* **93,** 071104 (2008).
27. Urbach, F. The long-wavelength edge of photographic sensitivity and of the electronic absorption of solids. *Phys. Rev.* **92,** 1324 (1953).
28. Wu, J. & Luo, F. Ultrafast femtosecond all-optical modulation through nondegenerate two-photon absorption in silicon-on-insulator waveguides. *J. Russian Laser Res.* **29,** 490–496 (2008).
29. Vahala, K. J. Optical microcavities. *Nature* **424,** 839–846 (2003).
30. Leuthold, J., Koos, C. & Freude, W. Nonlinear silicon photonics. *Nature Photon.* **4,** 535–544 (2010).
31. Apiratikul, P. & Murphy, T. E. Background-suppressed ultrafast optical sampling using nondegenerate two-photon absorption in a GaAs photodiode. *IEEE Photon. Technol. Lett.* **22,** 212–214 (2010).
32. Boitier, F., Dherbecourt, J. B., Godard, A. & Rosencher, E. Infrared quantum counting by nondegenerate two photon conductivity in GaAs. *Appl. Phys. Lett.* **94,** 081112 (2009).
33. Hayat, A., Ginzburg, P. & Orenstein, M. Infrared single-photon detection by two-photon absorption in silicon. *Phys. Rev. B* **77,** 125219 (2008).
34. Hayat, A., Ginzburg, P. & Orenstein, M. Observation of two-photon emission from semiconductors. *Nature Photon.* **2,** 238–241 (2008).
35. Delfyett, P. J. Optical frequency combs from semiconductor lasers and applications in ultrawideband signal processing and communications. *J. Lightwave Technol.* **24,** 2701–2719 (2006).
36. Chow, P. P. *et al.* Group III—nitride materials for ultraviolet detection applications. *SPIE: Optoelectronics Conference Proceedings*, 3948–32 (2000).

37. Pugh, S. K., Dugdale, D. J., Brand, S. & Abram, R. A. Electronic structure calculations on nitride semiconductors. *Semicond. Sci. Technol.* **14,** 23–31 (1999).
38. Bass, M., Li, G. & Van Stryland, E. W. *Handbook of Optics: Volume 4, Optical Properties of Materials, Nonlinear Optics, Quantum Optics* 3rd edn (McGraw-Hill, 2010).
39. Sheik-Bahae, M., Hutchings, D. C., Hagan, D. J. & Van Stryland, E. W. Dispersion of bound electronic nonlinear refraction in solids. *IEEE J. Quantum Electron.* **27,** 1296–1309 (1991).

## Acknowledgements

This work was supported in part by the US Army Research Office (grant no. 50372-CH-MUR) and the DARPA ZOE program (grant no. W31R4Q-09-1-0012).

## Author contributions

D.A.F., C.M.C., L.A.P. and S.W. conceived and performed the experiments. C.M.C and D.A.F. modelled the data and performed the theoretical analysis. M.M. designed and implemented the detection system. D.J.H. and E.W.V.S. suggested the basic concept of enhanced ND-2PA for experiments and applications. All authors contributed to the discussion of the results and writing the paper.

## Additional information

The authors declare no competing financial interests. Supplementary information accompanies this paper at www.nature.com/naturephotonics. Reprints and permission information is available online at http://www.nature.com/reprints. Correspondence and requests for materials should be addressed to E.W.V.S.